CHAPTER 2

PARP-2: Structure-Function Relationship

Valérie Schreiber, Michelle Ricoul, Jean-Christophe Amé, Françoise Dantzer, Véronique Meder, Catherine Spenlehauer, Patrick Stiegler, Claude Niedergang, Laure Sabatier, Vincent Favaudon, Josiane Ménissier-de Murcia and Gilbert de Murcia

Abstract

Poly(ADP-ribosyl)ation is an immediate DNA damage-dependent posttranslational modification of histones and other nuclear proteins that contributes to the survival of injured proliferating cells. Poly(ADP-ribose) polymerases (PARPs) now constitute a large family of 18 proteins, encoded by different genes and displaying a conserved catalytic domain in which PARP-1 (113 kDa), the founding member, and PARP-2 (62 kDa) are so far the sole enzymes whose catalytic activity is immediately stimulated by DNA strand-breaks. This review summarizes our present knowledge of the structure and function of PARP-2, the closest relative to PARP-1.

Abbreviations

PARP, poly(ADP-ribose) polymerase; XRCC1, X-ray cross complementing factor 1; BRCT, BRCA1 c-terminus; UVDE, UV damage endonuclease; GFP, green fluorescent protein; 3-AB, 3-aminobenzamide; XPA, xeroderma pigmentosum group A; DAPI, 4', 6-diamidino-2-phenylindol; TDT, deoxynucleotidyl transferase; PNK, polynucleotide kinase; MEFs, mouse embryonic fibroblasts; SSB, single strand breaks; SSBR, single strand breaks repair; DSB, double strand breaks.

Introduction

The presence of DNA strand breaks in the cells of higher eukaryotes activates signal transduction pathways that trigger cell cycle arrest and repair mechanisms leading ultimately to cell survival or programmed cell death. Changes in chromatin structure emanating from DNA breaks are probably the most initiating events in the cellular response to DNA damage. Central to pathways that maintain genomic integrity is the immediate modification of histones and nuclear proteins by ADP-ribose polymers catalyzed by poly(ADP-ribose) polymerases (PARPs).[1] A large repertoire of 18 sequences encoding novel PARPs now extend considerably the field of poly(ADP-ribosyl)ation reactions to various aspects of the cell biology including cell proliferation, cell death and energy metabolism. The members of the PARP superfamily are characterized by a conserved core with catalytic activity to which a number of specific targeting and regulatory modules have been added, leading to a spectrum of possible functions probably broader than genome surveillance (Amé et al submitted).

PARP-1 (113 kDa), the founding member, and PARP-2 (62 kDa) are so far the sole enzymes whose catalytic activity is immediately stimulated by DNA strand-breaks, suggesting that they are both involved in the cellular response to DNA damage. PARP-2 was discovered as a result of the presence of residual DNA-dependent PARP activity in embryonic fibroblasts

Poly(ADP-Ribosyl)ation, edited by Alexander Bürkle.

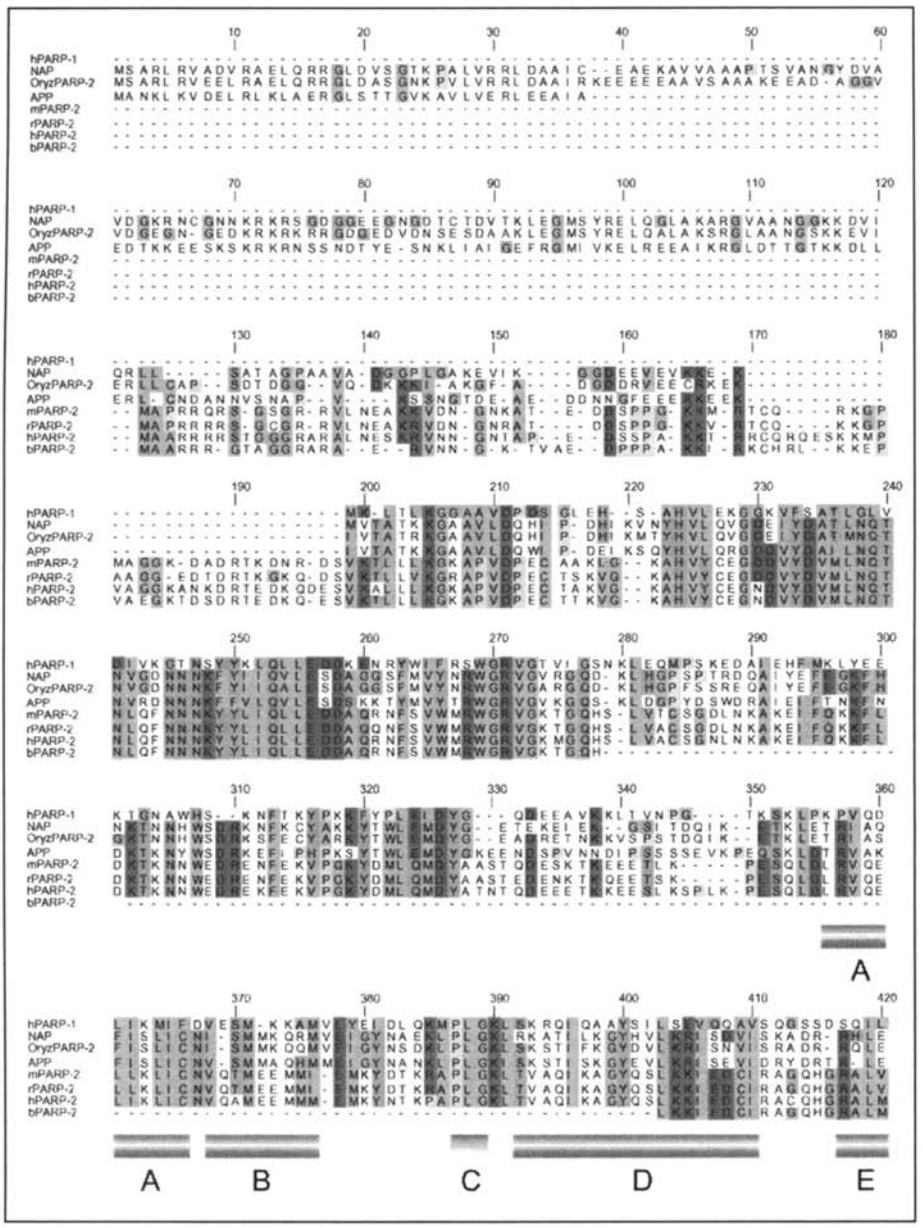

Figure 1. Sequence alignment of the deduced amino acid sequences of different PARP-2s with hPARP-1. Sequence alignment of human PARP-1 (hPARP-1, accession number P09874), human PARP-2 (hPARP-2, AJ236912), murine PARP-2 (mPARP-2, AJ007780), *Zea mais* NAP (AJ222588), *Arabidopsis thaliana* APP (Z48243), *Oryza sativa* PARP-2 (OryzPARP-2, NP_908921), *Rattus norvegicus* PARP-2 (rPARP-2, XP_214157), and partial sequence of bovine PARP-2 (bPARP-2). The amino acid color code is that of CLUSTALX (blue: >60% hydrophobics (ACFHILMVWY) ; Magenta: >50% negative charges (DE) ; Red : >60% positive charges (KR) ; Green : >50% polar (STQN) ; Pink : >85% cysteines ; Orange : >85% glycines ; Yellow : >85% prolines ; Cyan : >50% Aromatics (FYW). The secondary structure of the murine PARP-2 catalytic domain (aa 209-557) according to Oliver et al is shown. Continued on next page.

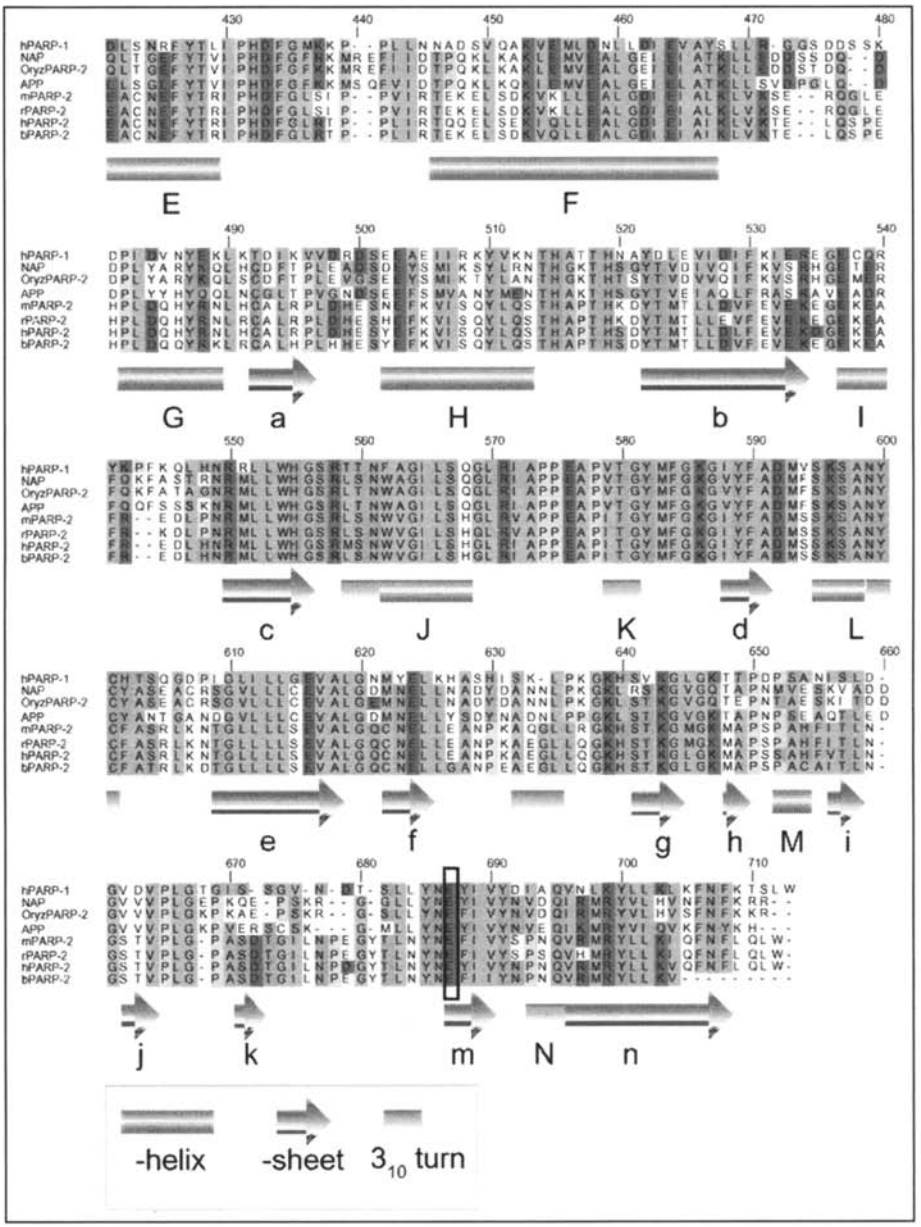

Figure 1, continued. A color version of this figure is available online at www.Eurekah.com.

derived from PARP-1 deficient mice.[2,3] This chapter summarizes the data obtained from molecular and genetic approaches developed in our laboratory to better understand the structure-function relationship of the mouse PARP-2.

PARP-2, the Closest PARP-1 Relative

Five years ago, we isolated a cDNA encoding a 62 kDa protein sharing considerable homology with the catalytic domain of PARP-1.[3] The assumption that we were dealing with a novel PARP enzyme was supported by the discovery in *Arabidopsis thaliana* of a gene coding for a PARP related polypeptide of a calculated mass of 72 kDa[4] and by the identification of two PARP homologues: one present at telomeres (Tankyrase 1)[5] and a second present in Vault particles (VPARP).[6] Hence, the protein encoded by this new cDNA was named PARP-2.

Figure 1 displays an alignment of seven PARP-2 translated cDNAs from plants and mammals. The N-terminal domain of PARP-2 (Fig. 2) comprising 65 residues in mouse supports several functions: it binds to DNA, it contains a nuclear targeting motif[3] and an interacting interface with the telomeric protein TRF2.[7] The PARP-2 DNA binding domain (DBD) displays some homology with the SAP domain[8] found in various nuclear proteins involved in chromosomal organization and in DNA repair such as AP-endonuclease and Ku70. The plant PARP-2 orthologues (*Arabidopsis thaliana* #NP_192148 and *Zea mais* #T03656) contain two SAP domains located at the N-terminus of the protein. A caspase-3 cleavage site located at the sequence ^{58}DNRD,^{61} defines the border between the DBD and domain E (homologous to the E domain of PARP-1).[9] Intriguingly, this caspase-3 cleavage site is not present in the rat nor in the bovine sequences (Fig. 1). Domain E acts both as an homodimerization interface and an automodification domain as well.[10] Among the PARP family members, PARP-2 is the closest relative to PARP-1, their catalytic domain (the F domain, Fig. 2) displays 69% similarity (see below). A caspase-8 cleavage site^{183}LQMD^{186} marks the border between domains E and F; the specific inactivation of PARP-2 at this conserved Bid-like site occurs in mice during middle cerebral artery occlusion.[11]

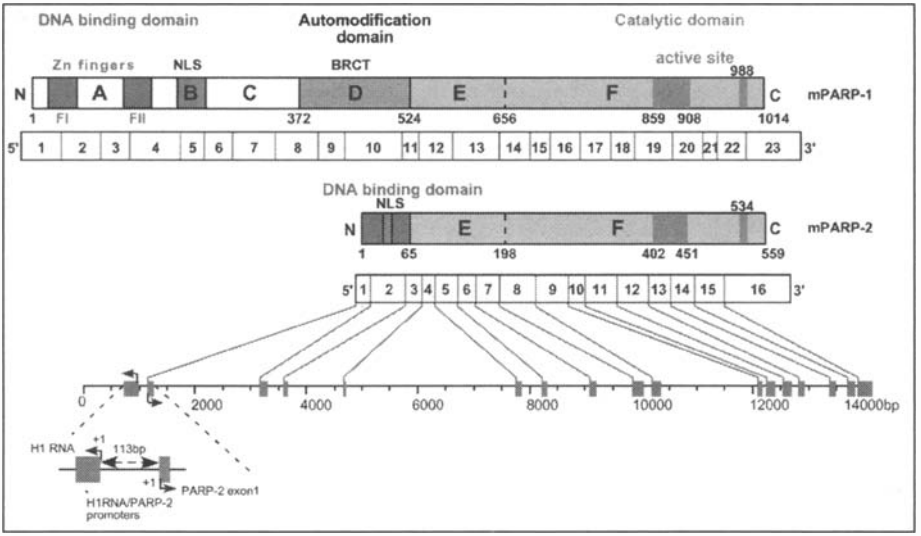

Figure 2. Structure of the mouse PARP-2 gene and comparison with the mouse PARP-1 exon organization. The gene structure is shown with length in bp, as deduced from Southern blot analysis with PARP-2 cDNA oligonucleotide probes. PARP-2 exons (1-16) as well as RNase P RNA (H1 RNA, GenBank accession number L08802) are represented as closed boxes. Mouse PARP-1 protein and its intron-exon organization has been aligned with the mPARP-2 protein. *NLS*, nuclear localization signal. (Taken from Amé et al,[3] with permission).

The PARP-2 gene located at position 14 q11.2 in human and 14 C1 in mouse consists of 16 exons and 15 introns spanning about 13 kilobase pairs (Fig. 2). Surprisingly, the PARP-2 gene lies head to head with the gene encoding the RNase P RNA subunit (H1 RNA). The distance between the transcription start sites of the PARP-2 and RNase P RNA genes is only 114 base pairs, suggesting that their regulation is coordinated through a bi-directional promoter. This unique promoter organization, conserved between human and mouse, allows an alternative gene expression mediated by RNA polymerase II (PARP-2) and by RNA polymerase III (H1 RNA) since they share common transcriptional control elements.[12] However, the expression of both genes is clearly independently regulated since PARP-2 is expressed at higher levels in proliferating cells of lymphoid organs, germinal cells, and duodenum epithelium in contrast to RNase P RNA which, as an essential gene, is ubiquitously expressed. Interestingly, ionising radiation strongly induces the expression of PARP-1 and PARP-2 genes in plants,[13] whereas the same genes are not inducible by DNA strand-breaks in mammals.

PARP-2, a Novel DNA-Damage Dependent Poly(ADP-Ribose) Polymerase

Affinity purified mouse PARP-2 (mPARP-2) overproduced in the Sf9 insect cells/baculovirus system displays DNA damage-dependent PARP activity. Using DNAse I treated DNA as a coactivator we estimated a K_m of 130 μM which represents an affinity for NAD^+ 2.6-fold lower than hPARP-1 (50 μM). The k_{cat}/K_m ratio (323 s^{-1} M^{-1}) is 18 times lower than that of hPARP-1, a value in good agreement with the 5-10% residual activity found in PARP-$1^{-/-}$ cell extracts stimulated by DNA strand breaks.[3]

The DNA-binding domain of mPARP-2 (aa 1-65; Fig. 2) was identified on the basis of its capacity to bind damaged DNA in a Southwestern assay.[3] Using precisely defined DNA ends, we demonstrated that purified mPARP-2 binds specifically to a gap of one nucleotide (Fig. 3A) and protects about 10 nucleotides. In contrast to PARP-1, PARP-2 does not bind to a break (Fig. 3B). The affinity of PARP-2 for the "inside" of the double helix can also be visualized by electron microscopy (Fig. 3C) where the protein accumulates and seems to displace one of the two DNA strands (arrows) when a break is present.

In the absence of any protein acceptor, PARP-2 can modify itself in vitro. Most of the radioactive label is found associated with domain E (aa 64-198) that is not only the PARP-2 automodification domain but also the interactive interface with partners like: PARP-1, XRCC1, DNA pol β, and DNA Ligase III. Domain E is also involved in PARP-2 dimerization.[10]

From reconstitution experiments where either purified PARP-1 or PARP-2 were mixed with purified nuclei from PARP-1 deficient cells (Fig. 3D), it can be inferred that PARP-1 preferentially poly(ADP-ribosyl)ates the linker histone H1, whereas PARP-2 modifies preferentially the core histone H2B. Therefore, PARP-1 and PARP-2 have different targets both in DNA and in chromatin further indicating that, as chromatin modifiers, they play specific functions.

The Crystal Structure of the Mouse PARP-2 Catalytic Domain: Differences and Similarities

The mouse PARP-2 catalytic domain (aa 198-559, domain F, Fig. 2) purified to homogeneity on a 3-aminobenzamide affinity column was recently crystallized (Fig. 4) at 2.8 Å resolution.[14] The PARP-2 catalytic domain consists of two main parts: an α-helical domain in N-terminal (aa 207-324) and a mixed α/β C-terminal domain (aa 332-557) containing the active site. As predicted from the homology with the corresponding region of PARP-1, the overall fold of PARP-2 catalytic domain is very similar to that of PARP-1, though with some interesting differences in the vicinity of the acceptor site (Fig. 4). The local environment of the acceptor site in PARP-2 is modified compared to that of PARP-1, mainly due to a 3 aa insertion in the loop connecting the β-strands *k* and *l* (in PARP-1). Within this loop particularly intriguing is the side chain of Y528, which has no equivalent in PARP-1 and points directly into the acceptor

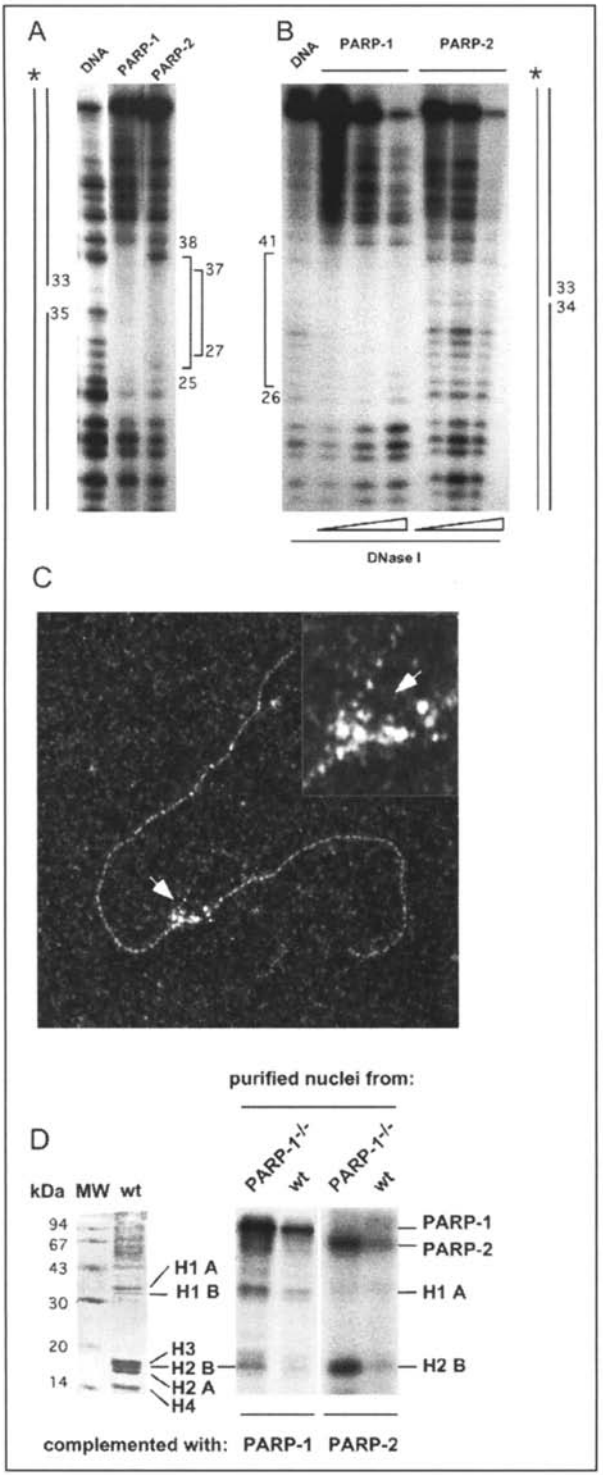

Figure 3. A) DNAse I footprinting of human PARP-1 and murine PARP-2 bound to a 66 bp DNA duplex containing a gap of one nucleotide located at position 33. The protection observed on the 5' end labelled continuous strand is indicated in brackets on the right. B) DNAse I footprinting of human PARP-1 and murine PARP-2 bound to a 66 bp DNA duplex containing a nick at position 33. No protection by mPARP-2 can be observed is this case. C) EM visualization of DNA strand displacement by mPARP-2 at a nick present on DNA (arrow). D) Auto and heteromodification reactions catalyzed by hPARP-1 and mPARP-2 following their introduction in purified nuclei from liver of wt or PARP-1 deficient mice.

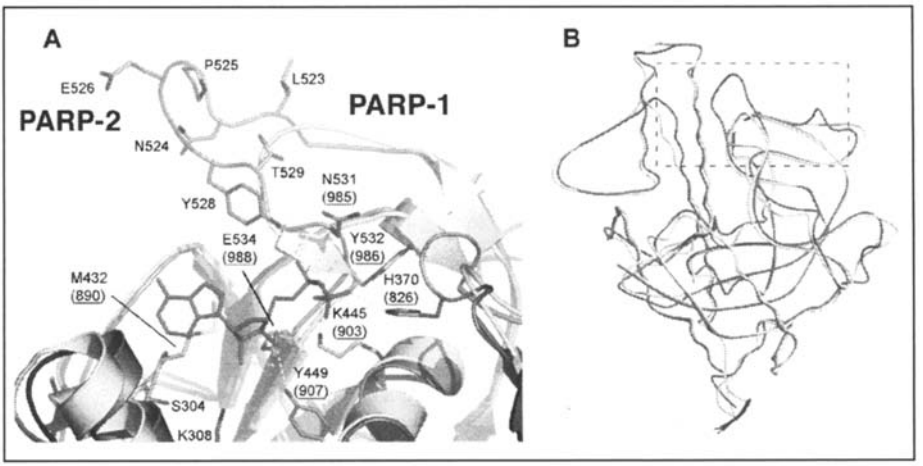

Figure 4. A) Poly(ADP-ribose) acceptor binding site. The ADP-ribose moiety (magenta) is shown bound to the donor site of PARP-1 (PDB:IEFY), along with a superimposition of the equivalent secondary structure elements in PARP-2.All residues involved in coordinating the substrate are highly conserved between the two PARP molecules. The extended loop (Leu 523- Thr529) unique to PARP-2 is clearly visible. In particular, residue Tyr528 is presented towards the acceptor site, possibly providing additional interactions with the pyrophosphate backbone of the bound substrate. Amino acid residues shown both in parentheses and underlined are in PARP-1. B) Superimposed Cα traces of PARP-1 (yellow) and PARP-2 (grey) catalytic fragments. The extended loop region is indicated in dotted line. (Taken from Oliver et al[14] with permission of Oxford University Press). A color version of this figure is available online at www.Eurekah.com.

site (Fig. 4A). This specific region is supposed to provide a binding site for the elongation of a terminal ADP-ribose of a growing polymer chain, or for the positioning of the acceptor glutamate in an initiation reaction. In view of the specificity of PARP-2 and PARP-1 towards different histones, it will be interesting to swap the loop between the two enzymes or to perform a mutational analysis of Y528, to test the influence of this region on the heteromodification reaction specificity.

Finally, the knowledge of the crystal structure of PARP-2 will certainly help in the development of specific inhibitors that may have also clinical applications as radiosensitizers (see below).

PARP-2 Localises Broadly across the Centromere during the Prometaphase and Metaphase Stages

Confinement of biomolecules within compartments is essential both for the formation and function of the cell. One of the major characteristics of the newly identified members of the PARP family is their various subcellular localizations. Figure 5 displays the subcellular localization of PARP-2 compared to that of PARP-1 in HeLa cells in various phases of the cell cycle. During interphase the accumulation of both PARP-1 and PARP-2 is clearly visible in the nucleoli of HeLa cells (panels 5A, 5F). PARP-1 has been shown to translocate from the nucleolus to the nucleoplasm when RNA synthesis is inhibited suggesting that its nucleolar location is dependent on the transcriptional state of the nucleolar chromatin.[15] It remains to see whether the same occurs with PARP-2.

Centromeres are the site of organization of kinetochores on mitotic chromosomes where chromosomes capture the spindle microtubules to ensure faithful chromosomal segregation during mitosis.[16] In mammalian cells, they span tens of megabases and are composed of large arrays of tandemly repeated sequences, the α-satellite in human and the minor satellite in

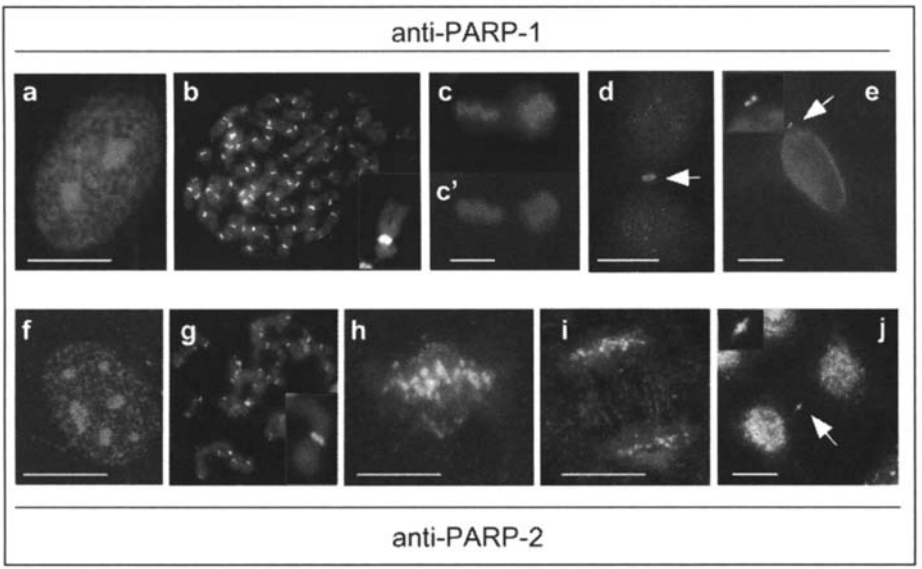

Figure 5. Subcellular immunolocalization of PARP-1 and PARP-2 : (a, e, f) interphase; (b, g) metaphase spreads; (c, c', h) metaphase; (i) anaphase; (d) early telophase; (j) late telophase. In b, g, h and i the image was merged with the CREST (centromeres) staining (green). The polyclonal antibodies anti-PARP-1 (a to e) and anti-PARP-2 (f to j) were labelled with an Alexa Fluor 568 goat anti-rabbit. Bars indicate 10 µm. A color version of this figure is available online at www.Eurekah.com.

mouse. While constitutive centromeric proteins, such as CENP-A, a histone H3-related protein, but also CENP-B or CENP-C remain centromeric throughout the cell cycle, some facultative centromeric proteins localise to kinetochore at specific stages during mitosis. This is the case for the spindle checkpoint protein BUB3 or the mitotic kinase Aurora B.[17]

As already described by the group of Choo and collaborators, PARP-1 [18] and PARP-2[19] are associated to the mammalian centromeres (panels 5B and 5G). Although in vitro affinity binding studies suggest that direct interaction with DNA sequences at centromeres and neocentromeres may be responsible for the recruitment of PARP-1 to centromeres, but sequence alone is clearly not sufficient for centromere localization. Identification of Cenpa, Cenpb and Bub3 as partners and possible poly(ADP-ribosyl)ated targets upon induction of DNA damage, has provided some insight into the function of PARP-1 at centromeres.[20] One can speculate that, following DNA strand breaks, PARPs may alter the kinetochore organization and affect the interaction of BUB3 with other checkpoint proteins involved in the spindle and anaphase progression. Localisation of PARP-2 at centromeres, in mouse and human cells suggest a significant functional role for two members (and perhaps more) of the PARP family at centromeres. Like PARP-1, PARP-2 binding is also linked with centromere activity rather than the underlying sequences.

The analysis of the distribution of both enzymes further in the cell cycle indicates a brief association of PARP-2 with the outer kinetochore at centromeres (inset panel G). In contrast to PARP-1 that stays on condensed chromatin during the next stages, i.e., metaphase and early anaphase (panels C and D), PARP-2 relocates to the spindle (panel H) and to the spindle midzone (panel I) and finally to the midbody (panel J) during cytokinesis. The dynamic association of PARP-2 with centromeres is therefore more akin to the previously described checkpoint proteins involved in spindle assembly. In line with this idea, the enhanced binding of PARP-2 to centromeres is observed when loss of spindle tension is induced by colcemid or taxol.[19]

Interestingly, during cytokinesis (panel D) a portion of PARP-1 localizes, differentially to PARP-2, to the actomyosin contractile ring (panel D) that needs to be resolved before the release of the intracellular bridge between two incipient daughter cells. Proteins at the midbody are known to provide molecular cues for the control of cytokinesis and the transition from mitosis to the next G1 phase. The presence of both PARP-1 and PARP-2 at kinetochores and their subsequent aggregation to the midbody suggest that they might play an important role as component of the cell cycle checkpoint machinery that regulates chromosome segregation during cell division. The localization of PARP-1 at the centrosome (panel E) further reinforces this proposal.

Radiosensitivity of PARP-2 Deficient Mice and Cells

To better understand the physiological role of PARP-2, the gene has been inactivated by homologous recombination in mouse embryonic stem cells (ES) by insertion of a PGK-hygromycin cassette.[9] To avoid any influence on the expression of H1 RNA , we chose to inactivate exon 9 at the corresponding position I_{285} of the aa sequence. Chimeric and mutant mice were obtained in C57BL6;129svPas mixed back-ground. Neither deregulation of RNase P RNA nor compensation by PARP-1 upregulation could be observed in Northern-blot analysis of total RNA isolated from testis. Mice lacking PARP-2 display no visible abnormal phenotype by 18 months of life and are not tumor-prone. However, in response to a whole body irradiation of 8 Gy they experienced a pronounced radiosensitivity and died (80% at two weeks after IR) from an acute radiotoxicity of the small intestine accompanied by a shortening of the villi and epithelial crypt degeneration. As shown in Figure 6A, PARP-2 deficient mice are however less radiosensitive than the PARP-1 deficient mice irradiated under the same experimental conditions.

The survival curves displayed in Figure 6B also demonstrate that, at the cellular level, the disruption of the PARP-2 gene sensitizes the cells to ionizing radiations. Interestingly, in the low-dose range (0-2 Gy, inset Fig. 6B) the PARP-2 deficient MEFs display a clear low-dose hyper-radiosensitivity (HRS) phenotype already described in wild-type cells irradiated with low doses of X-rays in the presence of various PARP inhibitors.[21,22] It is important to recall here that HRS is classically associated with a novel G2-phase arrest checkpoint that is specific for cells that are in the G2 phase of the cell cycle at the time of irradiation. Therefore, the absence of PARP-2 being clearly associated with a kinetochore defect, may well exacerbate HRS in the low-dose range, further pointing to possible clinical applications of PARP-2 inhibitors in combination with continuous low-dose rate radio-therapy.

The Physiological Role of PARP-2: A View from the Many Partners of PARP-2

To have a clue on the biological function of a protein, the elucidation of its proteic partners is worthwhile. Interestingly, PARP-1 was identified as the first partner of PARP-2.[10] The interaction between the two enzymes was revealed through co-immunoprecipitation experiments of Hela cell extracts but also with purified proteins, demonstrating a direct contact. The interaction is mediated by the BRCT and DNA binding domains of PARP-1 and the E domain of PARP-2. All these domains harbour auto- and heteromodification sites but polymer synthesis was not shown to significantly influence the interaction. PARP-2, like PARP-1, homodimerizes through its E domain. Homodimerization or heterodimerization seems to be a common feature of PARPs protein, since heterodimerization has been reported between PARP-3 and PARP-1,[23] or Tankyrase- 1 and -2.[24] It is also conceivable that PARP-1, the more active member of the family, is triggered at defined local sites were other less active PARPs reside, to amplify the cellular response to DNA damage. Whether and/or when PARP-2 acts as an heterodimer with PARP-1 or as homodimer is not understood yet. The two proteins follow comparable tissue distribution and subcellular localisation, and, even they may likely be involved in similar biological processes (see below), they could as well intervene at distinct steps in these processes.

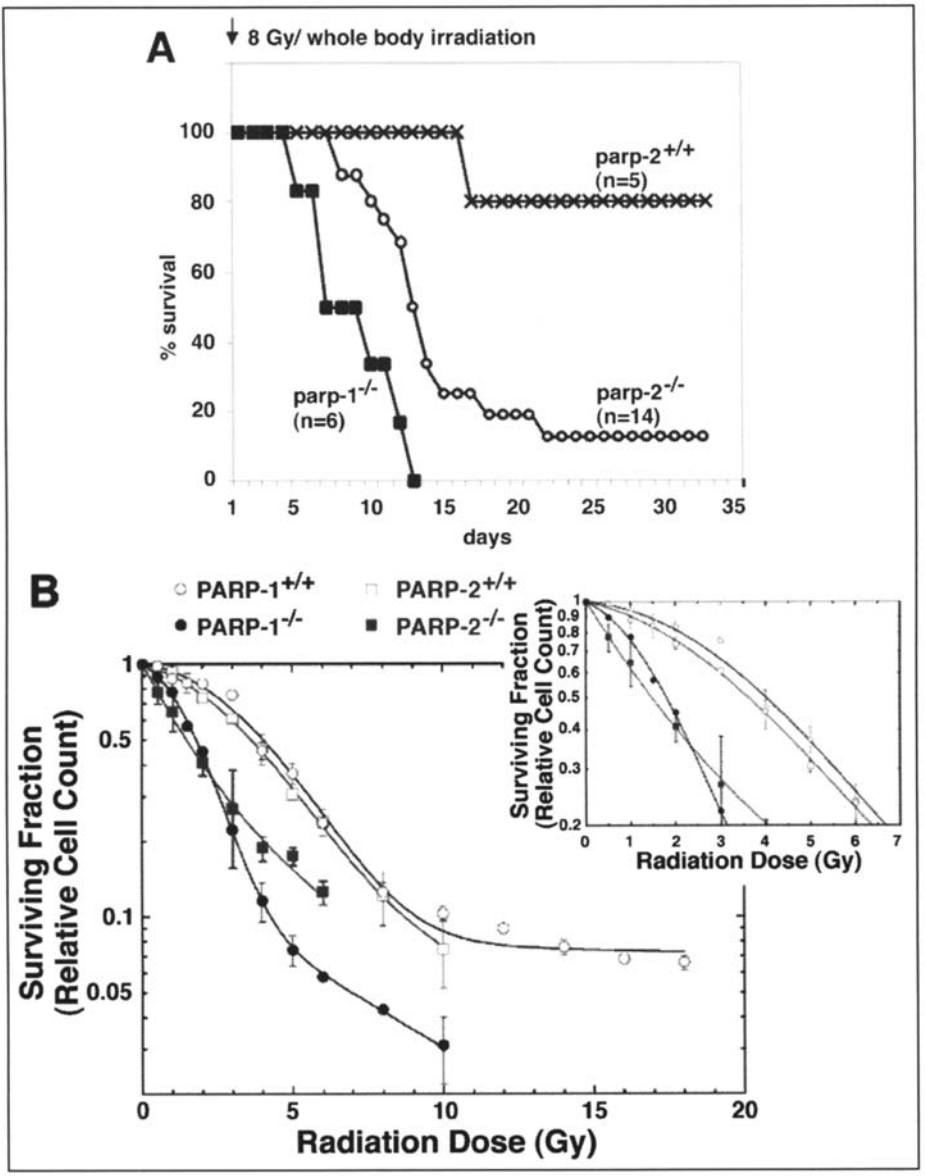

Figure 6. PARP-$2^{-/-}$ mice are sensitive to ionizing radiation. A) Kaplan-Meier survival curves after 8 Gy of whole body irradiation. Wilcoxon test : p(PARP-$2^{+/+}$ vs PARP-$2^{-/-}$)<10^{-5}. (Taken from Ménissier-de Murcia et al,[9] with permission). B) Comparison of γ-ray survival curves of wild-type, PARP-$1^{-/-}$ and PARP-$2^{-/-}$ mouse 3T3 fibroblasts. 10^5 fibroblasts from mid-log growing subcultures were plated in triplicate in 25 cm^2 flasks and returned to the incubator overnight prior to irradiation. Following treatment, the flasks were supplied with 8 ml fresh medium and grown for exactly 5 doubling times (relative to mock irradiated cells) with two changes of medium. Cells were harvested by trypsin-EDTA and scored visually under microscope. PARP-$1^{+/+}$, PARP-$1^{-/-}$ and PARP-$2^{+/+}$ fibroblasts yielded a convex curve which fitted a linear-quadratic dose-dependent equation, as most usually found among various cell lines, with a pseudo-plateau relating to G1 arrest. PARP-$2^{-/-}$ fibroblasts showed a concave profile and fitted a double-exponential equation. PARP-$2^{-/-}$ fibroblasts were clearly the most sensitive ones in the low dose range of radiation (insert) *Bars, SD.*

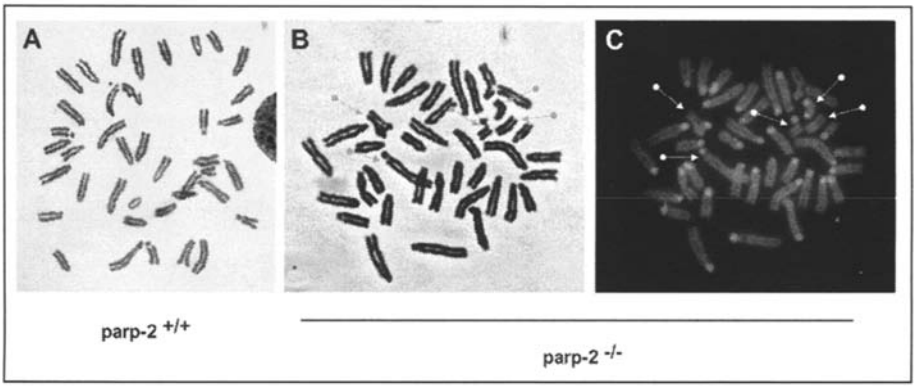

Figure 7. Occurence of chromatid breaks in centromeric region 7 h after 2 Gy irradiation. Metaphase spreads of bone marrow cells from irradiated PARP-$2^{+/+}$ (panel A) and PARP-$2^{-/-}$ mice (panel B-C). Arrows point to absence of centromeric signals. Giemsa staining (A,B); Chromosome painting with a centromeric probe, counterstaining with DAPI (C). (Taken from Ménissier-de Murcia et al,[9] with permission). A color version of this figure is available online at www.Eurekah.com.

PARP-2 and the Control of G2/M Transition of the Cell Cycle through Functional Kinetochore

As already mentioned above, the timing of the centromeric localization of PARP-2 differs from that of PARP-1 (Fig. 5): PARP-2 was first noticeable at centromeres during prometaphase, intensifying during metaphase, then disappearing from anaphase to telophase, a pattern of transient centromeric association resembling that of spindle assembly checkpoint proteins. It is worth mentioning that bone marrow cells from irradiated PARP-$2^{-/-}$ mice display an elevated number of chromatid breaks at the centromeric regions (Fig. 7), compared to wt cells. These observations suggest that PARP-2 is required at the kinetochore for the correct segregation of chromosomes during mitosis.[9] Indeed, the specific mis-segregation of the X-chromosome observed in PARP-$1^{+/-}$PARP-$2^{-/-}$ female embryonic fibroblasts could account for the female embryonic lethality of this genotype (see below). The treatment of PARP-$2^{-/-}$ cells with alkylating agents leads, 24 h after, to a G2/M cell cycle delay, with the appearance of polyploid cells (8N, Fig. 8A). This is accompanied by an increase in the proportion of aberrant anaphases (Fig. 8B). Immunofluorescent analyses using a CREST antibody to localise the centromeres revealed that a significant fraction of these aberrant anaphases displayed one or more lagging chromosome with centromeres mis-segregated between the two daughter cells (Fig. 8C). All these phenotypes observed in damaged PARP-$2^{-/-}$ cells reinforce the suggestive role of PARP-2 at centromeres and kinetochores, to ensure proper chromosome segregation during mitosis.[9]

PARP-2 in the Surveillance of Telomere Integrity

Telomeres, the extreme tips of chromosomes, consist of repetitions of T2AG3 DNA sequences in mammals (several kb or hundreds of kb in human and mouse, respectively) that erode with each cell cycle unless telomerase, a specialized reverse transcriptase resynthesises telomere repeats to maintain their length.[25] Together with their associated proteins, these sequences protect the chromosome ends from being considered as double strand breaks that would irremediably promote an inappropriate attempt to repair them by recombination mechanisms such as non homologous end-joining or homologous recombination.[26] Tankyrase-1 and -2 are telomeric PARPs that regulate telomere length through binding and poly(ADP-ribosyl)ation of the telomeric factor TRF1.[5,27] TRF2 has been shown to remodel telomeres into large duplex loops (t-loops) by the invasion of the 3' strand overhang into the duplex array of T2AG3 repeats.[28] The loss of telomere protection by TRF2 due to overexpression

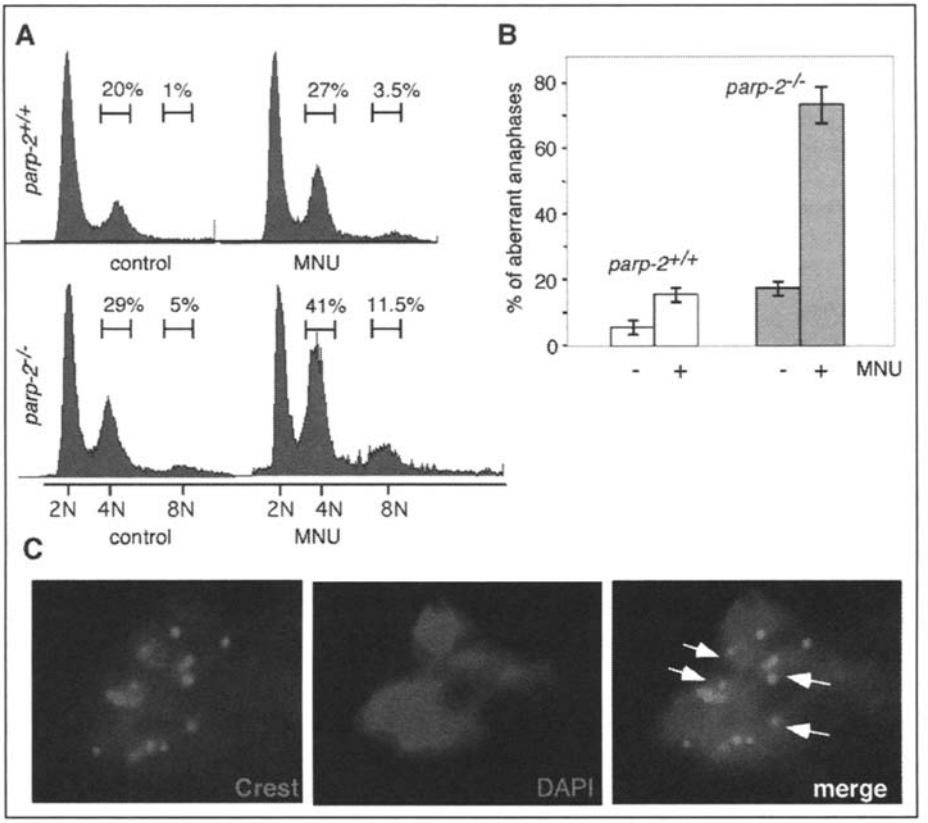

Figure 8. A) PARP-$2^{-/-}$ cells fail to resume their progression in the cell cycle following alkylating DNA base damage. Cell cycle profile analyzed after propidium iodide staining of PARP-$2^{+/+}$ and PARP-$2^{-/-}$ MEFs at passage 2, 24 h following 2 mM MNU treatment. The percentage of cells containing (2N) (4N) and (8N) is indicated. (Taken from Ménissier-de Murcia et al,[9] with permission.) B-C) Aberrant anaphases in PARP-$2^{-/-}$ cells following alkylating DNA base damage. Quantitative analysis of chromosome mis-segregation in PARP-$2^{+/+}$ and PARP-$2^{-/-}$ MEFs at passage 2, 24 h following 2 mM MNU treatment. The fraction of mitotic cells that exhibited a defect in segregation, such as lagging chromosomes is shown. Exemple of an anaphase of PARP-$2^{-/-}$ MEFs following 2 mM MNU treatment, with kinetochores immunostained with the CREST serum (red, left panlel) and DNA stained with Dapi (middle panel). A merged image is shown on the right panel. A color version of this figure is available online at www.Eurekah.com.

of a dominant-negative form of TRF2, results in end-to-end chromosome fusions and initiates a p53- and ATM-dependent apoptotic response.[29]

The possible participation of PARP-2 in the maintenance of telomere integrity was highlighted by the discovery of a functional interaction between PARP-2 and TRF2.[7] Both proteins were shown to strongly interact, through the N-terminal domain of PARP-2 and the myb DNA binding domain of TRF2. Neither DNA nor poly(ADP-ribose) was tethering the association of the two proteins. Interestingly, TRF2 could be poly(ADP-ribosyl)ated in vitro by PARP-2, and in addition, it could bind non covalently to poly(ADP-ribose) through its myb domain. Gel retardation assays (Fig. 9A) performed under conditions where both TRF2 (lane 3) and PARP-2 (lane 2) bound to the same target telomeric DNA probe revealed that the two proteins could bind simultaneously to the telomeric probe (lane 4).[7] Under conditions were PARP-2 is active in the presence of NAD+, TRF2 is released from the telomeric probe

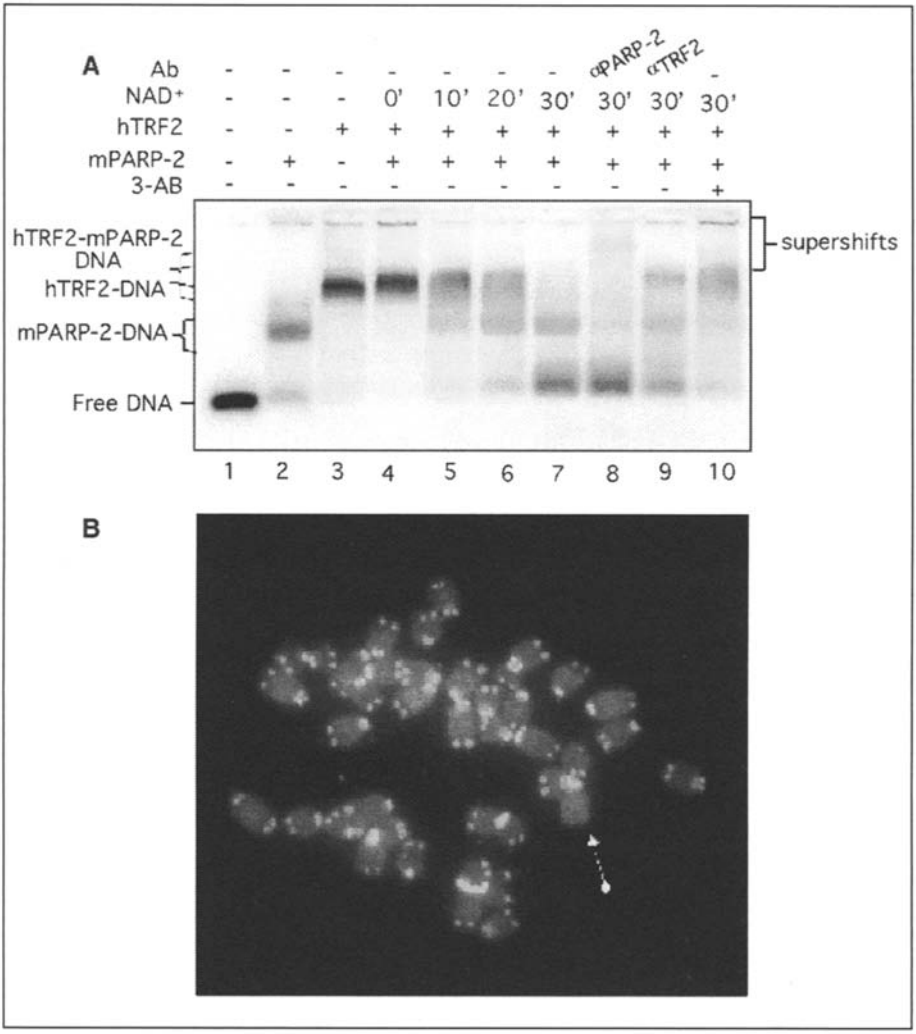

Figure 9. A) PARP-2 activity negatively regulates TRF2 DNA binding activity. The radiolabeled telomeric probe dsT4S1, containing 4 double stranded T2AG3 repeats and one 3'overhanging single strand repeat, was obtained by annealing a ^{32}P-end labeled 54-mer oligonucleoltide with the complementary 48-mer oligonucleotide. Purified hTRF2 (100nM) was preincubated with the radiolabeled telomeric probe under binding conditions at 20°C, and purified mPARP-2 (100 nM) was subsequently added for 10 min (lanes 4 to 10), followed by the addition of NAD+ for various times as indicated, in the absence (lanes 4 to 9) or in the presence of 3-AB (lane 10). In lanes 1 to 3, the radiolabeled telomeric probe was incubated with respectively no protein, mPARP-2 or TRF2 for 30 min under binding conditions. When indicated, antibodies against PARP-2 (lane 8) or TRF2 (lane 9) were added after 30 min incubation under binding conditions. The binding products were analyzed on a nondenaturing 1% agarose gel and phosphorimaging of the dried gel. The position of free DNA, complexes and supershifts are indicated. Note that the migration of the mPARP-2-hTRF2-DNA complex is only slightly retarded compared to that of the hTRF2-DNA complex. (Taken from Dantzer et al,[7] with permission of ASM Journals.) B) Chromosomal instability in PARP-2$^{-/-}$ primary MEFs. Quantitative fluorescence in situ hybridization (Q-FISH) analyses performed on PARP-2$^{-/-}$ MEFs metaphases. Signal free ends are indicated by arrows.

(lanes 5-7), whereas some PARP-2/DNA complex still remains. This is confirmed by the supershift observed with anti-PARP-2 (lane 8) but not with anti-TRF2 (lane 9) antibodies. In the presence of the PARP inhibitor 3-AB, TRF2 is not displaced anymore from the DNA probe (lane 10). These results indicate that poly(ADP-ribose) synthesis by PARP-2 negatively affects the binding of TRF2 to the telomeric DNA. Interestingly, poly(ADP-ribose) alone could also displace TRF2 from its telomeric substrate. Therefore, the inhibition of TRF2 DNA binding by PARP-2 involves both a covalent heteromodification of TRF2 and a non covalent binding of poly(ADP-ribose) to TRF2.

Attempts to colocalize PARP-2 and TRF2 in vivo were not successful in telomerase positive cell lines, possibly due to the abundant nuclear homogeneous distribution of PARP-2. However, in telomerase-negative cells that elongate their telomeres by an alternative mechanism (ALT), GFP-tagged mPARP-2 and TRF2 proteins were colocalized in some ALT-associated PML bodies (APB),i.e., nuclear substructures that harbor several players in DNA repair and recombination, such as RAD50/MRE11/NBS1, RAD52, RPA, BLM and WRN. In addition, poly(ADP-ribose) was also detected in these APB following cell exposure to hydrogen peroxide. It is tempting to speculate that PARP-2 could regulate the recombination-driven telomere synthesis in ALT cells through its association with TRF2.

The absence of PARP-2 in PARP-$2^{-/-}$ Mouse embryonic fibroblasts (MEFs) cells has no effect on mean telomere length measured by Q-FISH.[7] Telomerase activity is also unperturbed in these cells compared to wild type cells. However, there is a significant spontaneous increase in the signal-free ends in PARP-$2^{-/-}$ cells (Fig. 9B), as well as in the heterogeneity of telomere lengths per chromosome, in addition to an increase in the frequency of spontaneous chromosomes and chromatid breaks. These observations are suggestive of a telomere dysfunction in the absence of PARP-2.

Whereas Tankyrases 1 and 2 target TRF1 to monitor telomere length, one can assume that PARP-2 may target TRF2 to control telomere integrity and/or remodelling. It is also conceivable that PARP-2 activity could function at telomeres by modulating t-loop formation in response to DNA damage.

PARP-2: Another Actor in Base Excision Repair

PARP-2 together with PARP-1, are the only PARPs described until now that respond to DNA damage both in vivo and in vitro. A subset of PARP-2 proteic partners identified belong to the SSBR and BER machineries. GST-pull down analyses revealed that, in addition to PARP-1, XRCC1, DNA ligase III and DNA polβ could be copurified with the E domain of PARP-2.[10] The interaction between PARP-2 and XRCC1 was lost in the presence of the PARP inhibitor 3-AB, indicating that poly(ADP-ribose) synthesis is a prerequisite for XRCC1 binding to PARP-2, as well as to PARP-1, as previously reported.[30] Moreover, XRCC1 can be poly(ADP-ribosy)lated by PARP-2 and has the ability to negatively regulate PARP-2 activity, as it does with PARP-1.[10] All these biochemical data suggested that PARP-2 belongs to the SSBR/BER complex, together with PARP-1.

Further direct evidence came from in vivo studies on Mouse Embryonic Fibroblasts (MEFs) derived from PARP-2 knock-out mice (see below). The capacity of these PARP-2 deficient cells to repair DNA lesions induced by the alkylating agent MNU was evaluated in vivo using the single-cell gel electrophoresis assay (COMET assay). This technique can monitor the DNA strand breaks resealing in individual damaged cells as a function of time. Interestingly, PARP-$2^{-/-}$ cells display a considerable delay in strand breaks rejoining (2 h delay) compared with wt cells, but similar to that observed for PARP-$1^{-/-}$ cells (Fig. 10A).[10] Therefore, the absence of PARP-2 is as dramatic as the absence of PARP-1 despite the 10 times lower activity of PARP-2 in response to DNA damage, compared to PARP-1. This could be explained either by the disruption of the PARP-1/PARP-2 heterodimer in the absence of either PARP, or by the involvement of each PARP at distinct step of the SSBR/BER process. The elucidation of specific DNA substrates for each PARP would definitely clarify the latter hypothesis.

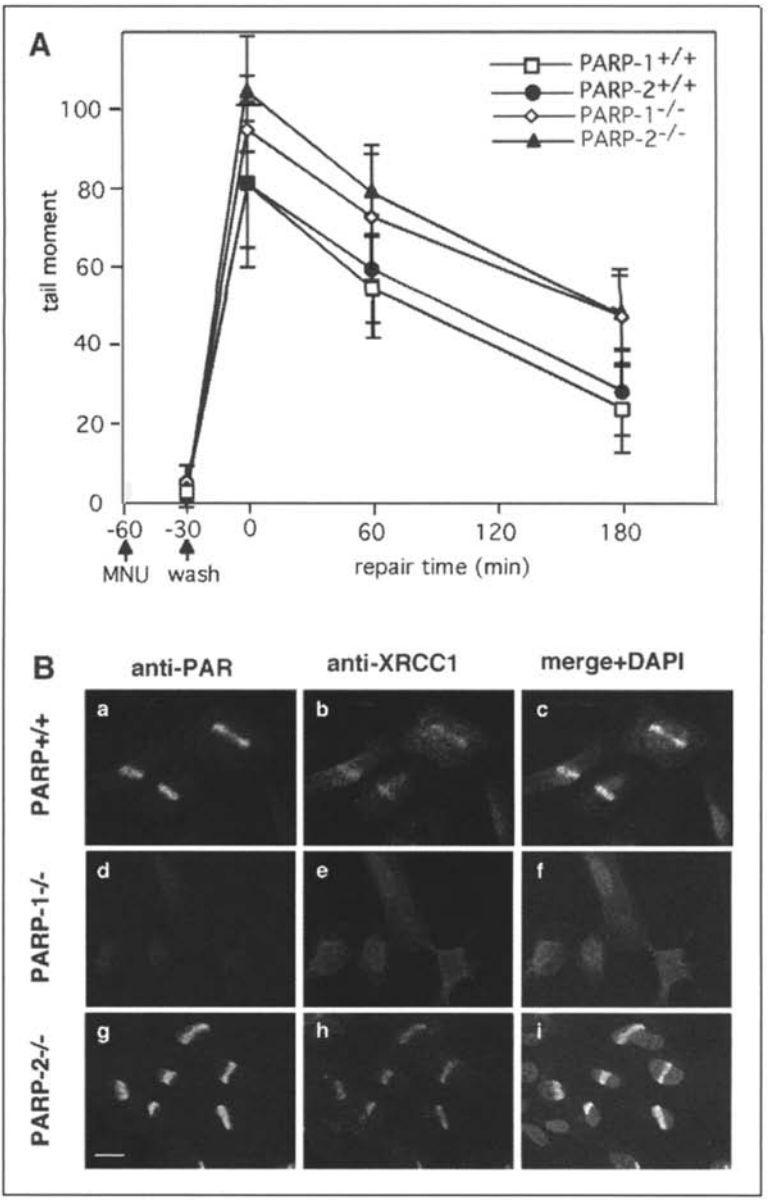

Figure 10. A) PARP-2 is required for efficient DNA repair of alkylated DNA in vivo. PARP-$2^{+/+}$, PARP-$2^{-/-}$, PARP-$1^{+/+}$ and PARP-$1^{-/-}$ MEFs were treated 30 min with 1 mM MNU and the kinetic of religation of DNA breaks was assessed by the COMET assay. The distribution of the tail moment as a function of repair time is indicated. (Taken from Schreiber et al,[10] with permission of ASBMB journals.) B) XRCC1 colocalizes with poly(ADP-ribose) synthesized by PARP-1 at laser-induced DNA breaks. Immortalized $PARP^{+/+}$ (a-c), PARP-$1^{-/-}$ (d-f) or PARP-$2^{-/-}$ (g-i) mouse embryonic fibroblasts were locally irradiated with UV-A laser microbeam (337 nm) in the presence of Hoechst 33258. Cells were fixed immediately and processed for immunostaining using anti PAR (a,d,g) and anti-XRCC1 (b,e,h). Images are merged together with the image of Dapi staining (c,f,i). A color version of this figure is available online at www.Eurekah.com.

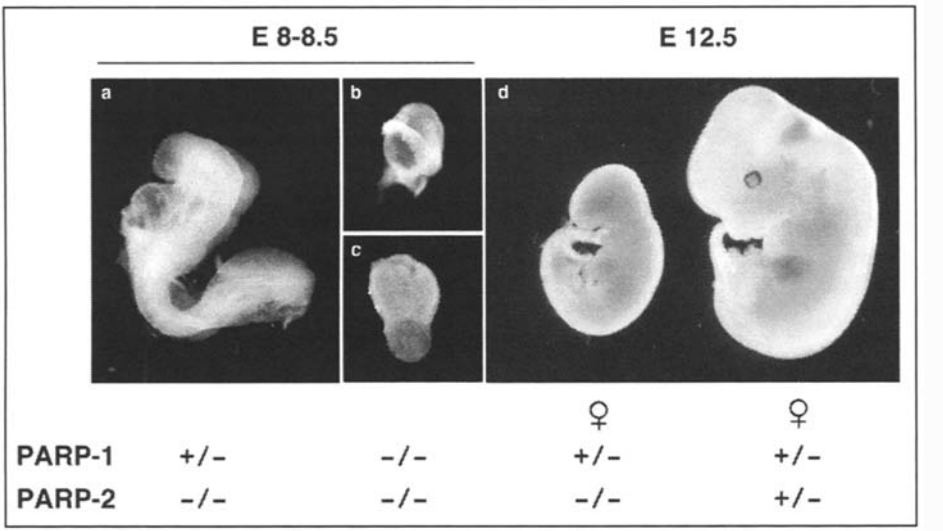

Figure 11. Two PARP-1 dosage-linked phenotypes in a PARP-2 null background : (b-c) early embryonic lethality at E 8-8.5 of double mutant (PARP-1 -/-;PARP-2-/-) embryos; (d) female lethality in PARP-$1^{+/-}$; PARP-$2^{-/-}$ embryos at E 12.5. (Taken from Ménissier-de Murcia et al,[9] with permission.)

The development of techniques allowing the introduction of DNA breaks at local sites were decisive to demonstrate the recruiting property of poly(ADP-ribose) synthesised at the damage site [31](Amé et al submitted). These DNA breaks were introduced either by UVA- laser microirradiation of Hoechst 33258-treated cells[32] or by UVC-irradiation in UVDE-expressing XPA cells. Poly(ADP-ribose) was synthesised locally along the laser path throughout the nuclei. XRCC1 was shown to accumulate at DNA breaks marked by polymer synthesis (Fig. 10B, a-c). When PARP activity was chemically inhibited (3AB or NU1025), XRCC1 did not accumulated anymore the laser path that could still be marked by γH2AX or by TdT labelling (Amé et al submitted).

To examine the contribution of PARP-1 and PARP-2 on the recruitment of XRCC1, wt, PARP-$1^{-/-}$ and PARP-$2^{-/-}$ 3T3 cells were microirradiated. While no recruitment of XRCC1 could be detected in most of the PARP-$1^{-/-}$ cells (Fig. 10B, d-f), an efficient recruitment of XRCC1 comparable to wt cells was still observed in PARP-$2^{-/-}$ cells (Fig. 10B, g-h). This result demonstrates that poly(ADP-ribose) synthesized by PARP-1 immediately triggers the rapid accumulation of XRCC1 at DNA breaks. Furthermore, this result strengthens the idea that PARP-2 is not involved in the DNA damage recognition step of SSBR/BER pathway, but in a subsequent step of the repair process, leading, when absent, to a repair defect as observed by the COMET assay.

What could be the step at which PARP-2 is required for efficient SSBR/BER? Identifying what is the DNA target of PARP-2, likely different to that of PARP-1 due to their distinct DNA binding domains is of particular interest to answer this question.

Conclusions and Perspectives

PARP-1 and PARP-2 clearly participate to the first line of defence of the genome as efficient DNA-break sensors and signaling molecules in a survival program, specific of higher eukaryotes. The ADP-ribose polymer they synthesize in response to DNA-interruptions plays a crucial role in the immediate recruitment of XRCC1 to the damaged sites. Confirmation of the importance in this function at the animal level is provided by the results from crosses of double heterozygote mice (PARP-$1^{+/-}$; PARP-$2^{+/-}$) telling us that double mutant mice are not viable and die at the onset of gastrulation (Fig. 11B,C). Thus, no other redundant function in vivo overcomes the

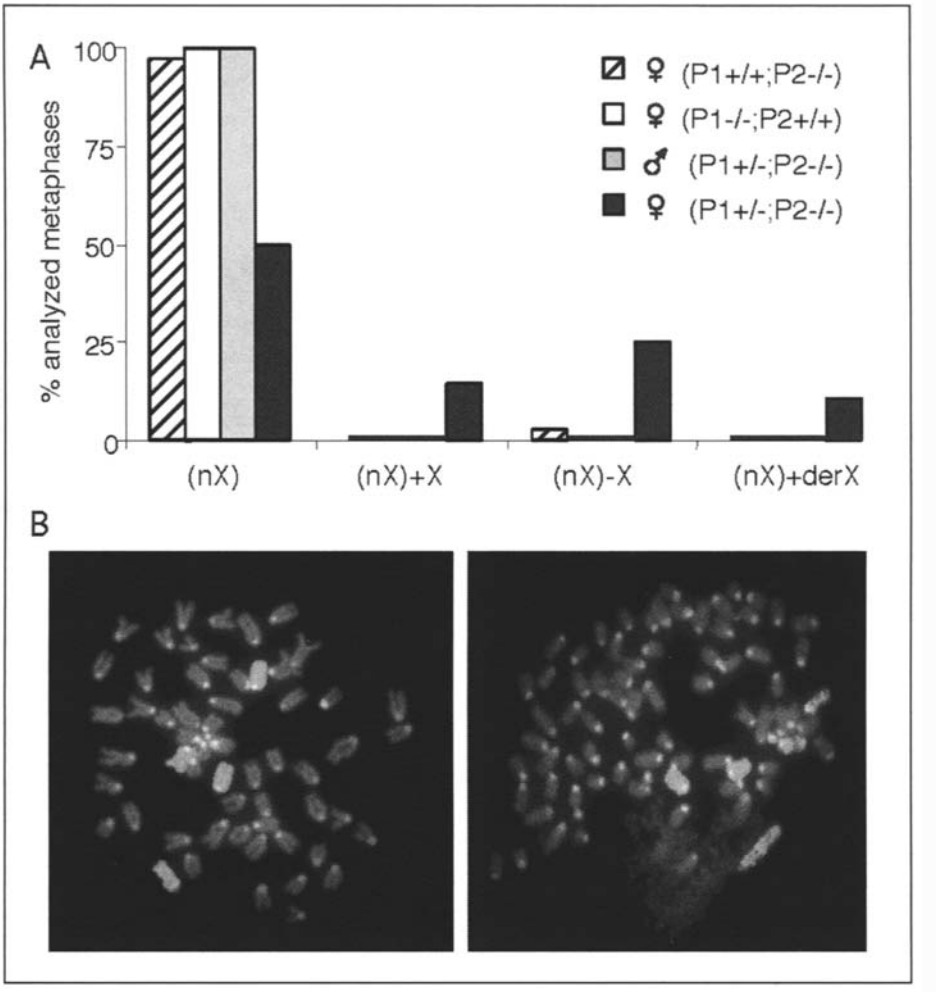

Figure 12. (PARP-$1^{+/-}$;PARP-$2^{-/-}$) female embryos display X-chromosome instability. A) Distribution of X-chromosome abnormalities in male and female embryos from various genotypes. B) Examples of metaphases with various numbers of X-chromosomes in (PARP-$1^{+/-}$;PARP-$2^{-/-}$) females. A color version of this figure is available online at www.Eurekah.com.

defect due to both (PARP-1;PARP-2) disruption. Lethality occuring shortly after gastrulation was also observed in mutant embryos lacking other BER factors such as XRCC[33] and APE.[34]

PARP-1 haplo-insufficiency in a PARP-$2^{-/-}$ context caused female-specific embryonic lethality (Fig. 11D) associated with X-chromosome instability (Fig. 12) indicating that in this setting half of the normal PARP-1 dosage in the absence of PARP-2 at centromeres induces a high frequency of kinetochore defects during X-chromosome segregation, thus increasing its well known lagging character. Alternatively, one could imagine that, as a silenced region of the genome, X-chromosome may be less frequently repaired than actively transcribed portions and therefore absolutely needs to be repaired during DNA replication to be faithfully transmitted. Depending on the extent of DNA damage, the inactivated X-chromosome might not be captured in time by the microtubules. This delay is most probably accentuated in the PARP-$2^{-/-}$ context, thus increasing its instability.

The presence of PARP-2 in regions of the genome containing repetitive DNA sequences like centromeres, telomeres and rDNA and in association with X-chromosomes suggest a role of PARP-2 in the maintenance of both constitutive and facultative heterochromatin integrity, which may become a target for pharmacological intervention.

Acknowledgements

We thank Dr. Sugimura for the 10H anti-poly(ADP-ribose) antibody. We are grateful to Didier Hentsch (IGBMC, Illkirch) and Jean-Christophe Laval (Leica Microsystems, France) for their help with the laser microbeam. This work was supported by funds from Centre National de la Recherche Scientifique, Association pour la Recherche Contre le Cancer, Electricité de France, Ligue Nationale Contre le Cancer and Commissariat à l'Energie Atomique.

References

1. de Murcia G, Shall S, eds. From DNA Damage and Stress Signalling to Cell Death: Poly (ADP-Ribosylation) Reactions. Oxford, New York: Oxford University Press, 2000:238.
2. Shieh WM, Ame JC, Wilson MV et al. Poly(ADP-ribose) polymerase null mouse cells synthesize ADP-ribose polymers. J Biol Chem 1998; 273(46):30069-72.
3. Ame JC, Rolli V, Schreiber V et al. PARP-2, A novel mammalian DNA damage-dependent poly(ADP-ribose) polymerase. J Biol Chem 1999; 274(25):17860-8.
4. Lepiniec L, Babiychuk E, Kushnir S et al. Characterization of an Arabidopsis thaliana cDNA homologue to animal poly(ADP-ribose) polymerase. FEBS Lett 1995; 364(2):103-8.
5. Smith S, Giriat I, Schmitt A et al. Tankyrase, a poly(ADP-ribose) polymerase at human telomeres. Science 1998; 282(5393):1484-7.
6. Kickhoefer VA, Siva AC, Kedersha NL et al. The 193-kD vault protein, VPARP, is a novel poly(ADP-ribose) polymerase. J Cell Biol 1999; 146(5):917-28.
7. Dantzer F, Giraud-Panis MJ, Jaco I et al. Functional Interaction between Poly(ADP-Ribose) Polymerase 2 (PARP-2) and TRF2: PARP Activity Negatively Regulates TRF2. Mol Cell Biol 2004; 24(4):1595-1607.
8. Aravind L, Koonin EV. SAP-a putative DNA-binding motif involved in chromosomal organization. Trends Biochem Sci 2000; 25(3):112-4.
9. Menissier de Murcia J, Ricoul M, Tartier L et al. Functional interaction between PARP-1 and PARP-2 in chromosome stability and embryonic development in mouse. EMBO J 2003; 22(9):2255-63.
10. Schreiber V, Ame JC, Dolle P et al. Poly(ADP-ribose) polymerase-2 (PARP-2) is required for efficient base excision DNA repair in association with PARP-1 and XRCC1. J Biol Chem 2002; 277(25):23028-36.
11. Benchoua A, Couriaud C, Guegan C et al. Active caspase-8 translocates into the nucleus of apoptotic cells to inactivate poly(ADP-ribose) polymerase-2. J Biol Chem 2002; 277(37):34217-22.
12. Ame JC, Schreiber V, Fraulob V et al. A bidirectional promoter connects the poly(ADP-ribose) polymerase 2 (PARP-2) gene to the gene for RNase P RNA. structure and expression of the mouse PARP-2 gene. J Biol Chem 2001; 276(14):11092-9.
13. Doucet-Chabeaud G, Godon C, Brutesco C et al. Ionising radiation induces the expression of PARP-1 and PARP-2 genes in Arabidopsis. Mol Genet Genomics 2001; 265(6):954-63.
14. Oliver AW, Ame JC, Roe SM et al. Crystal structure of the catalytic fragment of murine poly(ADP-ribose) polymerase-2. Nucleic Acids Res 2004; 32(2):456-464.
15. Desnoyers S, Kaufmann SH, Poirier GG. Alteration of the nucleolar localization of poly(ADP-ribose) polymerase upon treatment with transcription inhibitors. Exp Cell Res 1996; 227(1):146-53.
16. Choo KH. Domain organization at the centromere and neocentromere. Dev Cell 2001; 1(2):165-77.
17. Adams RR, Carmena M, Earnshaw WC. Chromosomal passengers and the (aurora) ABCs of mitosis. Trends Cell Biol 2001; 11(2):49-54.
18. Earle E, Saxena A, MacDonald A et al. Poly(ADP-ribose) polymerase at active centromeres and neocentromeres at metaphase. Hum Mol Genet 2000; 9(2):187-94.
19. Saxena A, Wong LH, Kalitsis P et al. Poly(ADP-ribose) polymerase 2 localizes to mammalian active centromeres and interacts with PARP-1, Cenpa, Cenpb and Bub3, but not Cenpc. Hum Mol Genet 2002; 11(19):2319-29.
20. Saxena A, Saffery R, Wong LH et al. Centromere proteins Cenpa, Cenpb, and Bub3 interact with poly(ADP-ribose) polymerase-1 protein and are poly(ADP-ribosyl)ated. J Biol Chem 2002; 277(30):26921-6.

21. Chalmers AJ. Poly(ADP-ribose) polymerase-1 and ionizing radiation: sensor, signaller and therapeutic target. Clin Oncol (R Coll Radiol) 2004; 16(1):29-39.
22. Chalmers A, Johnston P, Woodcock M et al. PARP-1, PARP-2, and the cellular response to low doses of ionizing radiation. Int J Radiat Oncol Biol Phys 2004; 58(2):410-9.
23. Augustin A, Spenlehauer C, Dumond H et al. PARP-3 localizes preferentially to the daughter centriole and interferes with the G1/S cell cycle progression. J Cell Sci 2003; 116(Pt 8):1551-62.
24. Sbodio JI, Lodish HF, Chi NW. Tankyrase-2 oligomerizes with tankyrase-1 and binds to both TRF1 (telomere-repeat-binding factor 1) and IRAP (insulin-responsive aminopeptidase). Biochem J 2002; 361(Pt 3):451-9.
25. de Lange T. Protection of mammalian telomeres. Oncogene 2002; 21(4):532-40.
26. Ferreira MG, Miller KM, Cooper JP. Indecent exposure: when telomeres become uncapped. Mol Cell 2004; 13(1):7-18.
27. Kaminker PG, Kim SH, Taylor RD et al. TANK2, a new TRF1-associated poly(ADP-ribose) polymerase, causes rapid induction of cell death upon overexpression. J Biol Chem 2001; 276(38):35891-9.
28. Griffith JD, Comeau L, Rosenfield S et al. Mammalian telomeres end in a large duplex loop. Cell 1999; 97(4):503-14.
29. van Steensel B, Smogorzewska A, de Lange T. TRF2 protects human telomeres from end-to-end fusions. Cell 1998; 92(3):401-13.
30. Masson M, Niedergang C, Schreiber V et al. XRCC1 is specifically associated with poly(ADP-ribose) polymerase and negatively regulates its activity following DNA damage. Mol Cell Biol 1998; 18(6):3563-71.
31. Okano S, Lan L, Caldecott KW et al. Spatial and temporal cellular responses to single-strand breaks in human cells. Mol Cell Biol 2003; 23(11):3974-81.
32. Rogakou EP, Boon C, Redon C et al. Megabase chromatin domains involved in DNA double-strand breaks in vivo. J Cell Biol 1999; 146(5):905-16.
33. Tebbs RS, Flannery ML, Meneses JJ et al. Requirement for the Xrcc1 DNA base excision repair gene during early mouse development. Dev Biol 1999; 208(2):513-29.
34. Ludwig DL, MacInnes MA, Takiguchi Y et al. A murine AP-endonuclease gene-targeted deficiency with post- implantation embryonic progression and ionizing radiation sensitivity. Mutat Res 1998; 409(1):17-29.